

AD-779 412

PRECISION TRANSONIC BAROMETRIC FUZE
SYSTEM FOR THE LASER GUIDED HONEST
JOHN MISSILE

Irvin Pollin

Harry Diamond Laboratories
Washington, D.C.

August 1973

DISTRIBUTED BY:

NTIS

National Technical Information Service
U. S. DEPARTMENT OF COMMERCE
5285 Port Royal Road, Springfield Va. 22151

Reproduced by
NATIONAL TECHNICAL
INFORMATION SERVICE
U S Department of Commerce
Springfield VA 22151

UNCLASSIFIED

Security Classification

AD-79412

DOCUMENT CONTROL DATA - R&D		
<i>(Security classification of title, body of abstract and indexing annotation must be entered when the overall report is classified)</i>		
1 ORIGINATING ACTIVITY (Corporate author) Harry Diamond Laboratories Washington, DC 20438		2a REPORT SECURITY CLASSIFICATION Unclassified 2b GROUP
3 REPORT TITLE PRECISION TRANSONIC BAROMETRIC FUZE SYSTEM FOR THE LASER GUIDED HONEST JOHN MISSILE		
4 DESCRIPTIVE NOTES (Type of report and inclusive dates)		
5 AUTHOR(S) (Last name, first name, initial) Irvin Pollin		
6 REPORT DATE August 1973	7a TOTAL NO OF PAGES	7b NO OF REFS 29
8a CONTRACT OR GRANT NO	9a ORIGINATOR'S REPORT NUMBER(S) HDL-TR-1646	
b PROJECT NO DA-1X263306D073 AMCMS CODE: 523F.46.15600	9b OTHER REPORT NO(S) (Any other numbers that may be assigned this report)	
c HDL Proj: 41443	d	
10 AVAILABILITY LIMITATION NOTICES Approved for Public Release; Distribution Unlimited		
11 SUPPLEMENTARY NOTES	12 SPONSORING MILITARY ACTIVITY MICOM	
13 ABSTRACT For application to the proposed laser guided Honest John missile barometric fuze system, specially designed probes to measure the undisturbed free-stream ambient pressure were mounted forward of the nose of a full-scale model of the missile forward section and tested in the Naval Ship Research and Development Center's 7x10 ft transonic wind tunnel facility at Mach numbers 0.90 to 1.15 and at an approximately constant Reynolds number per foot of 1.92 million, the latter corresponding to an altitude of approximately 40,000 ft. Test data was obtained for the after body angle of attack range 0 to 10 degrees with 0 and 15 degree canard deflections. For the above conditions, the pressure probe is capable of measuring altitude to within ±100 ft and the fuze system is capable of measuring altitude to within ±120 ft. Although it is expected that the above precision can be maintained for altitudes between sea level and 5,000 ft, additional wind tunnel tests at the appropriate Reynolds numbers are required.		
Reproduced by NATIONAL TECHNICAL INFORMATION SERVICE U S Department of Commerce Springfield VA 22151		Details of illustrations in this document may be better studied on microfiche.

DD FORM 1 JAN 68 1473

UNCLASSIFIED
Security Classification

UNCLASSIFIED

Security Classification

14	KEY WORDS	LINK A		LINK B		LINK C	
		ROLE	WT	ROLE	WT	ROLE	WT
	Transonic Altimeter Barometric Fuze						

UNCLASSIFIED

Security Classification

AD

DA-1X263306D073
AMCMS Code: 523F.46.15600
HDL Proj. No. 41443

HDL-TR-1646

**PRECISION TRANSONIC BAROMETRIC FUZE SYSTEM
FOR THE LASER GUIDED HONEST JOHN MISSILE**

by
Irvin Pollin

August 1973



U.S. ARMY MATERIEL COMMAND,
HARRY DIAMOND LABORATORIES
WASHINGTON, D.C. 20438

APPROVED FOR PUBLIC RELEASE; DISTRIBUTION UNLIMITED.

ACKNOWLEDGEMENT

The support provided by Mr. Virgil S. Ritchie of NASA, Langley through his guidance, constructive suggestions, and technical review of the paper and the loan of probe A by NASA, Langley is greatly appreciated.

CONTENTS

	<u>Page</u>
ABSTRACT.....	1
ACKNOWLEDGEMENT.....	4
1. INTRODUCTION.....	7
2. APPARATUS.....	11
2.1 Wind Tunnel and Measurement Precision.....	11
2.2 Test Model.....	13
2.3 Position Error Probe.....	13
2.4 Compensation Probes.....	13
2.5 Dummy Probe.....	18
3. DETERMINATION OF AMBIENT PRESSURE.....	19
3.1 Position Error Measurements.....	19
3.2 Compensation Probe Measurements.....	28
4. SUMMARY.....	36
SYMBOLS.....	38
LITERATURE CITED.....	39
APPENDIX.....	43

FIGURES

1A. Forward section of the Laser Guided Honest John Missile..	7
1B. Compensation and dummy probes mounted on the nose of the Laser Guided Honest John Missile.....	10
2. Reynolds numbers of NSRDC tests and for flight at standard atmospheric conditions.....	11
3. Position error probe.....	14
4A. Compensation probe A.....	15
4B. Compensation probe B.....	16
4C. Compensation probe C.....	17
5. Dummy probe.....	18
6. Flow field around nose of missile. Mach number = 1.024	20

FIGURES (Cont.)

Page

7.	Flow field around nose of missile. Mach number = 1.137.....	20
8.	Position error measurements for probe mounted along missile axis showing effect of canard and afterbody deflections at various locations forward of the missile nose.....	22
9.	Position error measurements for probe mounted on the side of the missile nose for several locations forward of the missile nose.....	23
10.	Position of bow shock on position error probe. M = 1.003.....	25
11.	Position of bow shock on position error probe. M = 1.011.....	26
12.	Position of bow shock on position error probe. M = 1.019.....	27
13.	Position of bow shock on position error probe. M = 1.030.....	29
14.	Position of bow shock on position error probe. M = 1.049.....	30
15A.	Error in measuring undisturbed free stream ambient pressure. Probe A.....	32
15B.	Error in measuring undisturbed free stream ambient pressure. Probe B.....	33
15C.	Error in measuring undisturbed free stream ambient pressure. Probe C.....	34

1. INTRODUCTION

The Laser Guided Honest John Missile is provided with a seeker nose swiveled to the vehicle afterbody, (fig. 1A). The seeker nose, essentially a hemisphere-circular cylinder of diameter 3.3 in., is provided with a ring-tail which causes the seeker nose to self-align with the flight velocity vector. The stagnation region of the nose is provided with laser optics and the radome glass eye enclosing the optics has an aperture of about 1.3 in. For guidance, canards attached to an afterbody are deflected through $+5$ degrees with respect to the afterbody, and the afterbody can attain angles of incidence of $+10$ degrees with respect to the seeker nose.



Figure 1A. Forward section of the Laser Guided Honest John Missile

The fuzing requirement specifies the determination of an altitude within the range sea level to 5000 ft, with a 3 sigma system precision of 200 ft. The method of determining the fuzing altitude is accomplished by sensing the value of the undisturbed ambient pressure when the vehicle is at the required altitude over the target at a speed between Mach 0.9 and 1.2. The error budget is assumed to be comprised of the errors arising from the following sources:

- (a) Prediction of the pressure-altitude relationship over the target,
- (b) Time response of the system, relating to the difference in time between that at which the pressure is sensed at the orifices to the closing of a barometric switch,
- (c) Barometric switch closure, and
- (d) Sensing the undisturbed ambient pressure.

In evaluating altitude error, it will be convenient to refer to the fact that for all altitudes between sea level and 5,000 ft, a 1-percent variation of pressure corresponds to an altitude change of about 275 ft. Accordingly, the magnitudes of these errors appear to be as follows:

The pressure-altitude relationship at the launch site is assumed known to within the accuracy of a balloon measurement. Horizontal pressure gradients over flat, unchanging terrains are generally negligible over distances of 15 miles. Consequently, the error in the predicted pressure-altitude relation at the target is assumed to be 0.1 percent of the actual undisturbed ambient pressure.

It is assumed that the vertical rate of descent of the vehicle over the target does not exceed 1,000 ft/sec. The length of the air line as measured from the sensing orifices to the barometric switch will be about 2 ft. Since a prediction of the pressure variation with time over the target can be included in reducing the time lag error and because the air line diameter can be modified as required, it is assumed that the time lag response error can be limited to 10 msec, (refs 1-3).^{*} The corresponding altitude error thereby does not exceed 10 ft.

Barometric switches with fixed pressure settings are production items and are readily available to determine a pressure with an accuracy of 0.25 percent, (ref 4).

Each of the four sources of error mentioned above occurs independently of the other. The principal source of error is in the sensing of the undisturbed ambient pressure. Consequently, in order to attain the required ± 200 ft accuracy, the undisturbed ambient pressure must be sensed to within 0.7 percent of its value.

^{*}Literature Cited is listed on pages 39, 40, and 41.

The technology and hardware for producing the required barometric fuze system are available for all items except the pressure sensor. Since a moving vehicle alters the pressure field of the enveloping fluid, the requirement of a precision pressure sensor means that this device must be adapted to the specific vehicle and its trajectory. Accordingly, an "off-the-shelf" precision pressure sensor is not possible and it was necessary to develop a sensor specifically adapted for the Laser Guided Honest John Missile. This development consisted primarily in the wind tunnel testing of previously tested bodies. Previous work to develop precision pressure sensors to measure undisturbed ambient pressure over a range of transonic Mach numbers is given in references 5-20. The sensor development presented here follows precisely the procedure described in reference 5.

The problem of developing a precision pressure sensor to determine undisturbed ambient pressure for a Mach number range consists of two parts:

- (a) Locating the orifices in the pressure field influenced by the vehicle motion such that the pressure at the site of the orifices can be established as a known, well-behaved, unique function of the vehicle Mach number, and
- (b) Designing a compensation probe on which the orifices are located so that, at each Mach number, the pressure induced by the probe at the site of the orifices is equal and opposite to that produced by the moving vehicle.

The pressure change (with respect to the undisturbed ambient) caused by the vehicle motion, noted in (a), is called "the position error." The position error is used to establish the requirements for the compensation probe. When the position error is known, the problem remains to find the body, i.e., the compensation probe shape, having the characteristics described above. Because of possible flow angularity, the orifices are circularly distributed and the compensation probe is a body of revolution. As will be indicated, the pressure sensor may be completely evaluated in a wind tunnel and flight tests may not be necessary.

Two probes, symmetrically mounted, will be used in the flight application, (fig. 1B). The longer probe is the compensation probe and the shorter probe is used to maintain a balance in the aerodynamic drag so as to allow the seeker nose to align with the wind velocity vector.

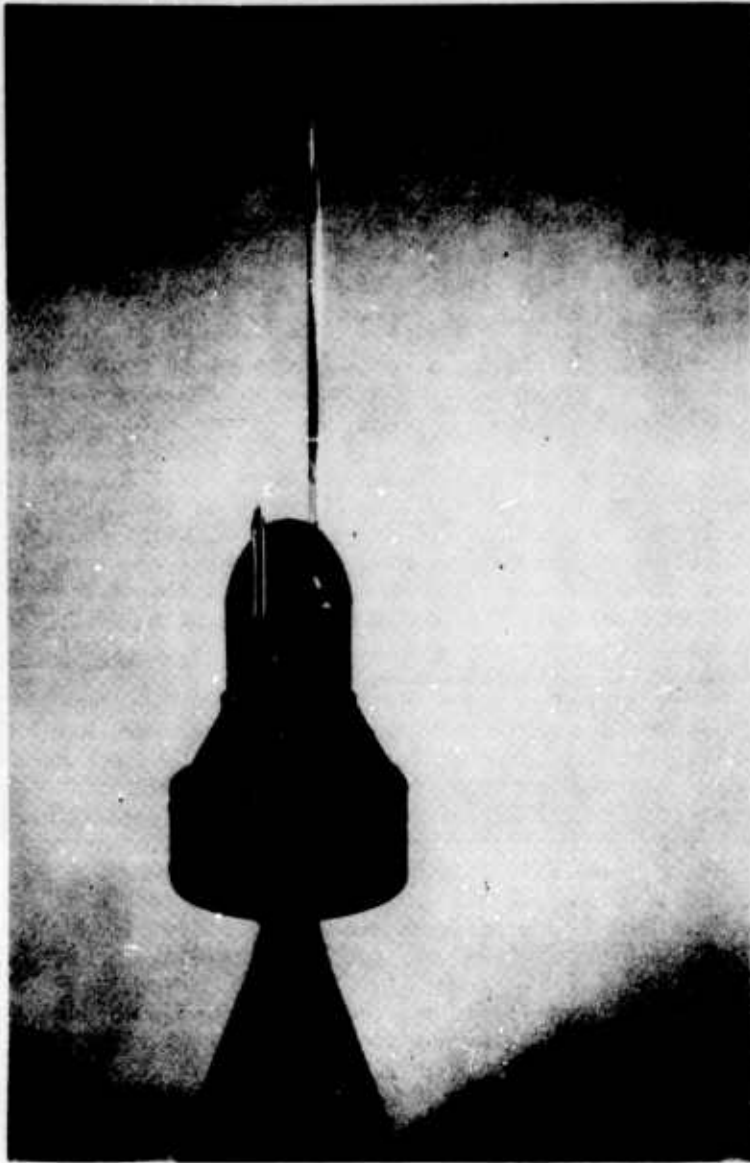


Figure 1B. Compensation and dummy probes mounted on the nose of the Laser Guided Honest John Missile

2. APPARATUS

2.1 Wind Tunnel and Measurement Precision

All test data was obtained in the continuous 7 x 10 ft NSRDC transonic wind tunnel facility (refs 21, 22). The test Mach number range 0.90 to 1.15 was obtained by altering the fan speed and venting the test section pressure. The associated Reynolds number per foot for all tests was approximately 1.92 million, which corresponds to an altitude of approximately 40,000 ft. As shown in figure 2, the Reynolds numbers of the NSRDC facility are smaller than those corresponding to flight conditions by a factor of between 3 and 4.

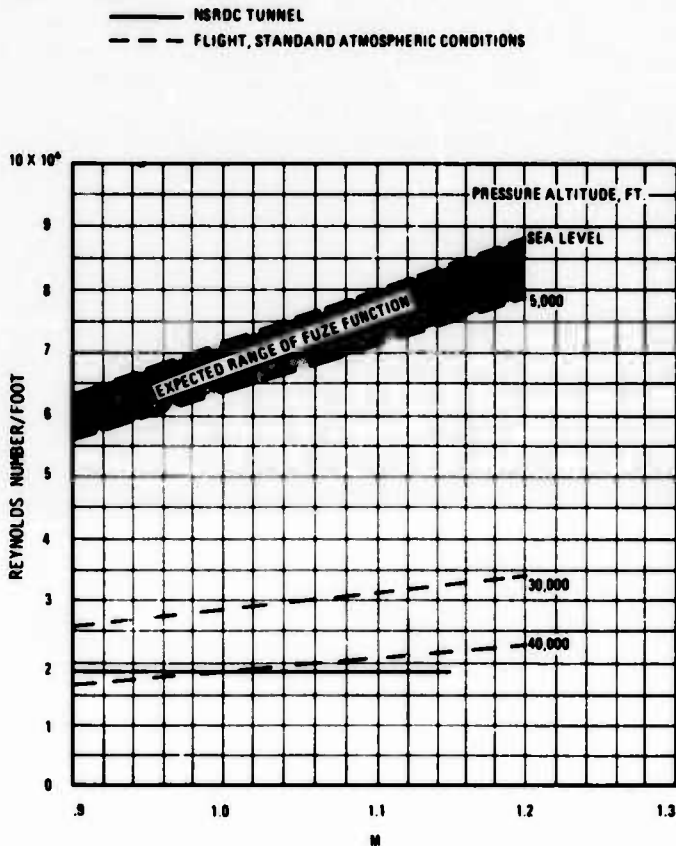


Figure 2. Reynolds numbers of NSRDC tests and for flight at standard atmospheric conditions

For all tests, temperature-calibrated pressure transducers having a full-scale range of ± 1 psi, with a maximum error of 0.005 psi over the entire pressure range, were used to measure the test section total pressure at the model and the static pressures on the position error and compensation probes. The test section total pressure transducer was referenced to the total in the wind tunnel settling chamber and the static pressures were referenced to the tunnel static in the tank. (The lower and upper tank sections are the sections below and above the slots in the floor and ceiling of the test section.) The reference readings were measured by an electronic liquid manometer which has an accuracy of ± 0.001 psi. The wind tunnel free stream static pressures ranged in value between 3.1 and 4.0 psi, so that the maximum 0.005 psi transducer error corresponds to a maximum error of 0.16 percent of the undisturbed ambient pressure. However, as determined from the transducer calibrations, observing the transducer repeatability, and comparing the data output of transducers simultaneously subjected to the same pressure, it appears that the actual measurement error caused by the transducers is within 0.1 percent of the wind tunnel free stream static pressure.

Except for boundary reflected shocks, the static pressures in the test section along the tunnel centerline are always within 1 percent of the tunnel static pressure. However, the relation between the static pressures along the tunnel centerline with the tunnel reference static is not known. (The determination of this relation is a major task of reference 22.) The present data assumes that the centerline pressures are the same as the tunnel tank (reference) static.

The small wind tunnel flow misalignment, less than 0.5 degree, is not a source of error in the probe measurements because the probe orifices are in a circular ring and connected to a common chamber at each station.

The blockage of the model for zero deflection of the canards and afterbody amounted to 0.6 ft^2 and increased for maximum deflections of these surfaces to 0.8 ft^2 . Thus, for all tests, the blockage amounted to only about 1 percent of the tunnel test section area; no blockage corrections were made.

Accounting for the above sources of error, the maximum measurement error in determining the probe static pressures amounts to 0.1 percent of the wind tunnel free stream static pressure. The maximum error in measuring the total pitot pressure at the model amounted to 0.1 percent of the wind tunnel total pressure. For speeds in the Mach range 0.90 to 1.15, an 0.1 percent error in measuring static or total pressure produces an approximately 0.1 percent error in the determination of Mach number.

2.2 Test Model

All tests were made using a full-scale, production model of the forward section of the Laser Guided Honest John Missile, (fig. 1). The section tested is sufficiently large to yield the same induced pressures forward of the nose as would occur for the entire vehicle. This fact was demonstrated experimentally by showing that the induced pressures occurring forward of the nose for zero canard and afterbody deflections were within 0.1 to 0.2 percent of those obtained for fully deflected canards and afterbody.

2.3 Position Error Probe

The position error probe consisted of a circular-cylindrical stainless steel tube, 0.375 in. in outside diameter, with an open-ended blunt nose to measure pitot pressure, (fig. 3). The orifices were set in rings of 8 orifices each, with adjacent orifices spaced 45 degrees apart, at stations 4.5, 6.5, 8.5, and 9.5 in. aft of the nose. All orifices had a diameter of 0.031 inch. All orifice stations were located 12 or more probe diameters downstream of the nose and therefore, since the probe was aligned with the flow velocity vector, the pressures at these stations were local static pressures not measurably influenced by disturbances at the nose or otherwise by the presence of the probe.

The position error probe was provided with five internally sealed chambers so that the pitot pressure and four static pressures could be measured simultaneously; each static pressure was the average value at the station given by a ring of orifices. Tubing of 0.10 in. inside diameter of approximately 2 ft lengths was used to connect each chamber with a transducer.

2.4 Compensation Probes

The three compensation probes used in the tests are illustrated in figures 4A, 4B, and 4C and their coordinates are given in the appendix. Probe A is the probe 1A cited in reference 5. A feature of this probe is the four rings of orifices axially spaced to attempt to minimize the effect of the bow shock.

The coordinates of probe B were obtained by changing the scale of the probe described with $A_{base}/A_{max} = 0.532$, $l/d_{max} = 13$ and with a ring of orifices at $x/l = 0.305$; see p. 11 of reference 6. This probe is illustrated in figure 4B and the coordinates are given in the appendix.

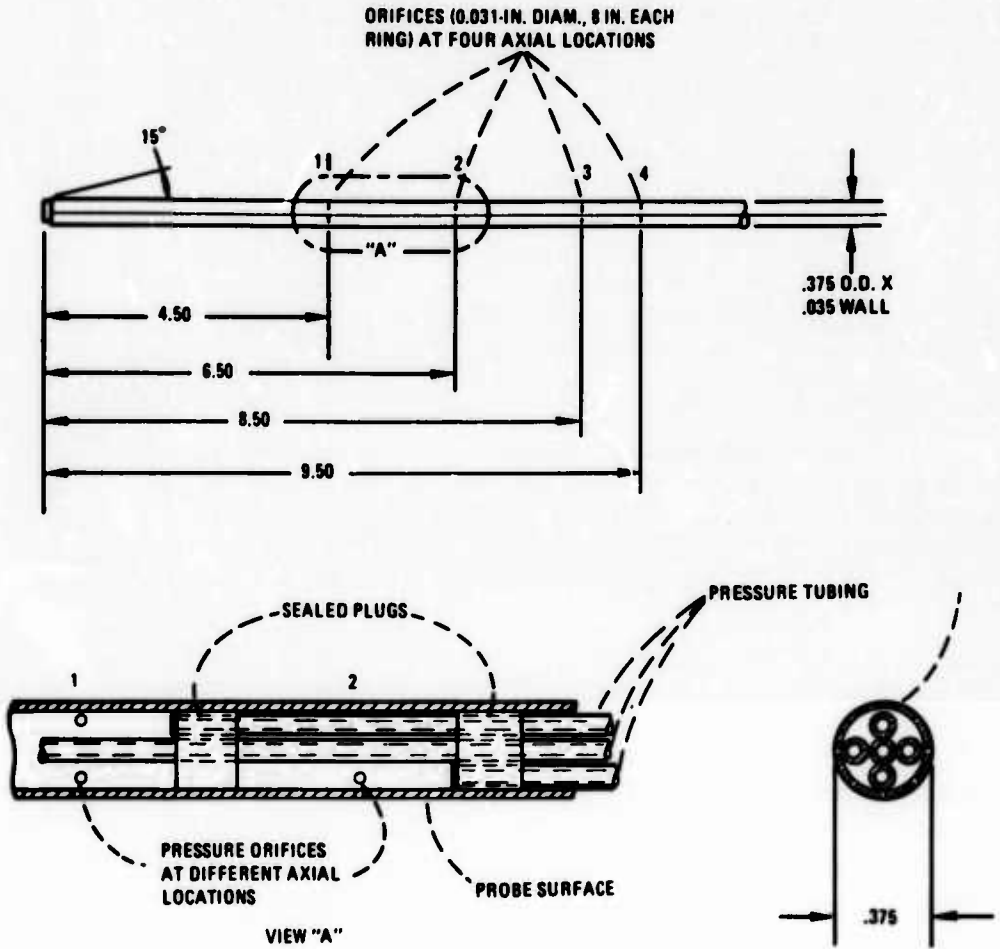


Figure 3. Position error probe

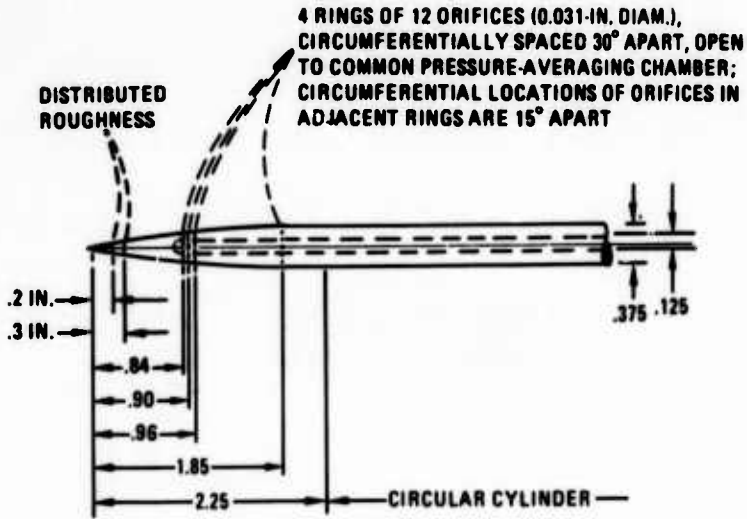


Figure 4A. Compensation probe A

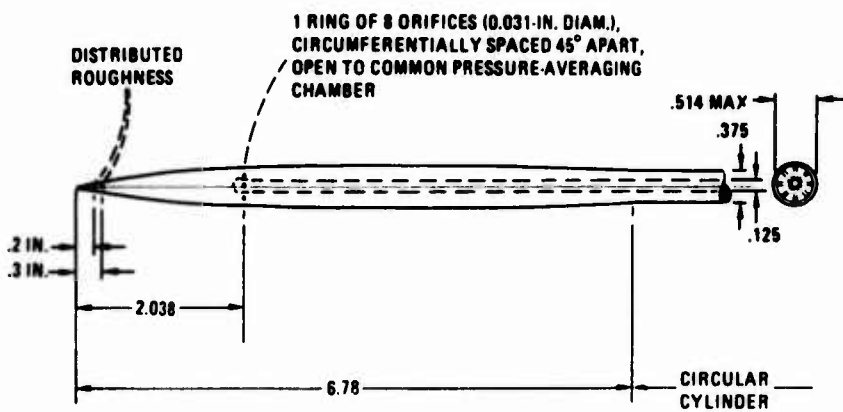


Figure 4B. Compensation probe B

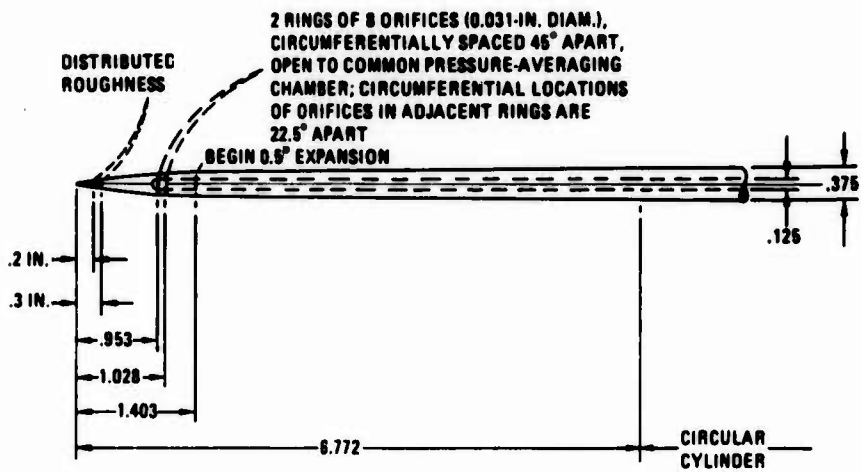


Figure 4C. Compensation probe C

The coordinates of probe C were obtained by scaling a probe design for which unpublished wind tunnel data is available, (fig. 4C). The nose section of this probe is a circular arc, followed by a truncated conical section whose generators make an angle of 0.5 degree with respect to the probe axis. Upon attaining an outer diameter of 0.375 in., the conical section changes into a circular cylinder.

The orifices for all probes were 0.31 in. in diameter and were connected to a common chamber. This chamber consisted of the inside tubing of the probe. In this way, errors arising from possible small flow angularities were reduced.

The surfaces of all compensation probes were highly polished and free of burrs and irregularities near the orifices, except for distributed roughness about 0.005 in. high located between stations 0.2 and 0.3 in. aft of the nose tip. The purpose of the roughness was to fix boundary layer transition, (ref 23).

2.5 Dummy Probe

A dummy probe to balance the aerodynamic drag arising from the compensation probe and thereby to help maintain the vehicle nose self-alignment with the velocity vector was mounted with the dummy probe nose extending 1 in. forward of the vehicle nose, (fig. 1B). In the wind tunnel tests, a blunt tipped probe, rather than the pointed one shown, was used to measure local pitot pressure and thus provide a check on the total pressure measurements recorded in the tunnel settling chamber. Construction details of this probe are given in figure 5.

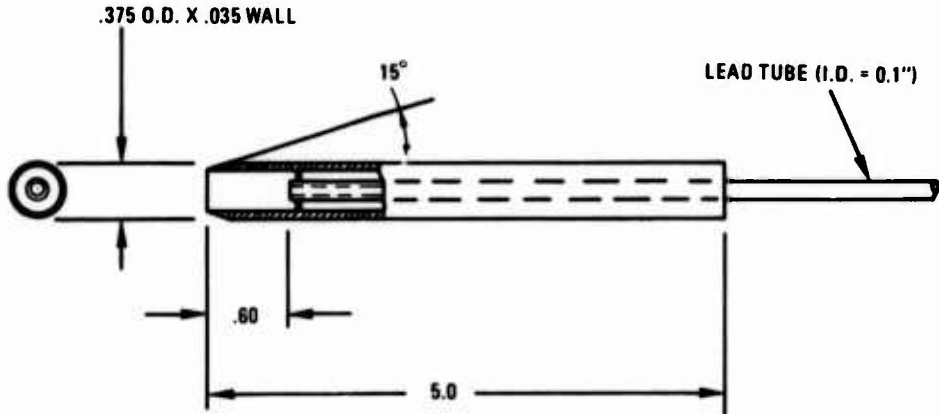


Figure 5. Dummy probe

3. DETERMINATION OF AMBIENT PRESSURE

3.1 Position Error Measurements

The pressure variation with Mach number at any point on a surface of a vehicle easily exceeds +20 percent of the average value at that point over the Mach range 0.9 to 1.2, (refs 24-29). Flow separation and shocks, acting alone or in combination, together with large changes in local velocity produce large variations of static pressure. Schlieren photographs of the Honest John Missile taken at Mach 1.024 and 1.137 clearly illustrate this type of flow, (figs. 6 and 7). The local Mach number varies from 0 at the stagnation point to almost twice that of the vehicle at a short distance aft of the stagnation point. The isentropic variation of stagnation pressure amounts to +18 percent through the speed range Mach 0.90 to 1.20. Consequently, it is not possible to determine the undisturbed ambient pressure to a precision of say +10% by locating a pressure sensor on the Honest John vehicle itself.

The pressure is larger than the undisturbed ambient for subsonic speeds at stations forward of the vehicle nose, and this difference increases with increasing Mach number and with decreasing distance from the nose, (ref 5). At very low supersonic speeds, the flow is supersonic (and equal to that of the vehicle) at distances of several nose diameters forward of the vehicle, followed by a shock, called the bow shock, and is subsonic between the bow shock and the nose. The Mach number gradient along the nose axis is continuous from the nose to the bow shock. At Mach 1.01, the bow shock oscillates in position between 3 and 4 nose diameters forward of the nose. As the vehicle speed further increases, the bow shock proceeds towards the nose and the strength of the shock increases (ratio of pressures behind to forward of the shock). The pressure everywhere forward of the bow shock is the undisturbed ambient pressure.

A precision probe thereby requires that the orifices be located where the error produced by the shock is within the application precision requirements. Once this requirement is met, the compensation probe is designed to induce a pressure (with respect to the undisturbed ambient) equal and opposite to that induced by the vehicle when the orifices are in a subsonic flow field and no pressure change at supersonic speeds, the latter occurring when the bow shock is between the orifices and the nose.

Small bow shock strengths not exceeding 1.005 (ratio of downstream to upstream static pressures across the shock) require orifice locations of 2 or more nose diameters forward of the nose. Moreover, it is easier to design a compensation probe and more precise measurements of ambient pressure at transonic speeds are usually possible when the

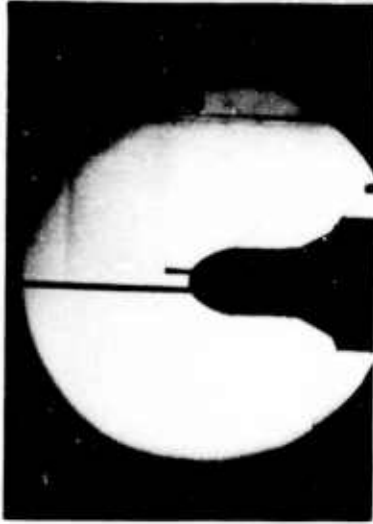


Figure 6. Flow field around nose of missile. Mach number = 1.024

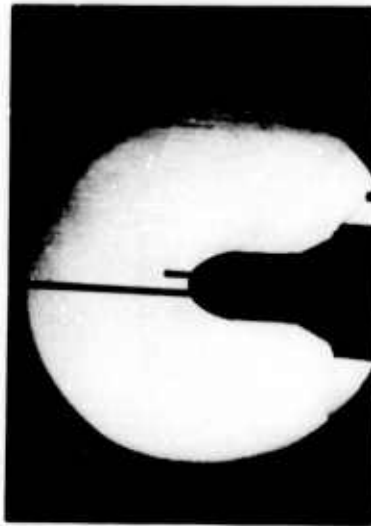


Figure 7. Flow field around nose of missile. Mach number = 1.137

magnitude of the required subsonic induced pressure is small. Thus, the probe precision improves as the orifices are placed farther forward of the nose.

The position error probe, previously described, measures the true static pressure simultaneously at each of the four axial positions of the orifices. The position error probe was mounted with its axis along the vehicle nose axis and measurements were obtained through the Mach range 0.90 to 1.00 for afterbody angles of incidence between 0 and 10 degrees with 0 and 5 degree canard deflections. The orifices were located 5, 6, 8, and 10 in. forward of the nose. At subsonic speeds, deflections of the canards and afterbody tend to increase the static pressure at the above orifice positions.

The data given in figure 8 clearly shows that this anticipated static pressure increase amounts to only about 0.1 to 0.2 percent for all orifice locations throughout the entire Mach range. Of course, as previously noted, the canard and afterbody deflections have no effect when the orifices are in a supersonic flow. For all practical purposes, this means that the performance of the position error and compensation probes can be evaluated for a single configuration of the vehicle.

For the above tests, it may be worth noting that the nose was free to swivel and self-align with the air stream. In each test, the nose aligned to within 0.2 degree of the tunnel axis, which was the limiting accuracy of this measurement. In all of the remaining test work, for convenience and to insure flow alignment, the seeker nose was locked into position and the canards were set at 5 degrees with zero afterbody deflection.

For flight application, the compensation probes are expected to be mounted on the side of the nose and not along the nose axis, figure 1. Consequently, in all the remaining tests, the position error measurements given in figure 9 and compensation probe measurements were obtained for the probes mounted on the side of the nose, as designed for use in actual flight. As experimentally demonstrated in reference 5 and as indicated by the close agreement between the data of figures 8 and 9 the pressure gradient normal to the nose axis is negligibly small at distances of two or more nose diameters forward of the nose.

In actual flight, to help maintain the required nose self-alignment with the velocity vector, it is expected that the compensation probe will be used together with a dummy probe mounted on the side of the nose and rotated 180 degrees from the compensation probe. The main aerodynamic contribution of the compensation probe is expected to be the drag produced at the junction of the probe with the nose. Accordingly, as a dummy, all test measurements were made using the 3/8 in. diameter pitot pressure probe mounted with the nose tip of the probe 1 in. forward of the vehicle nose.

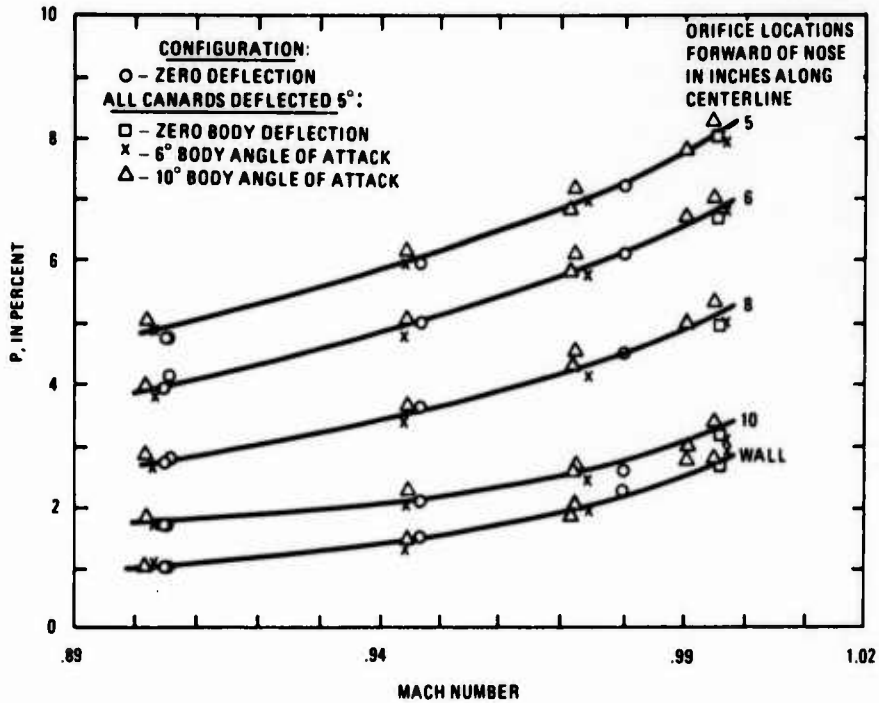


Figure 8. Position error measurements for probe mounted along missile axis showing effect of canard and afterbody deflections at various locations forward of the missile nose

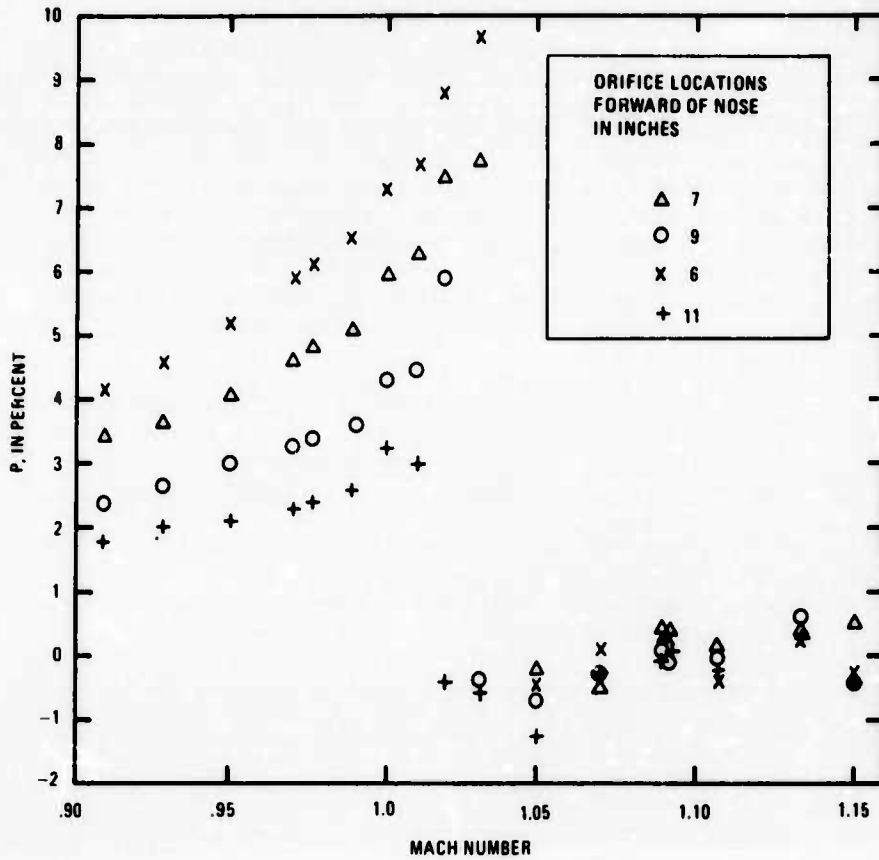


Figure 9. Position error measurements for probe mounted on the side of the missile nose for several locations forward of the missile nose.

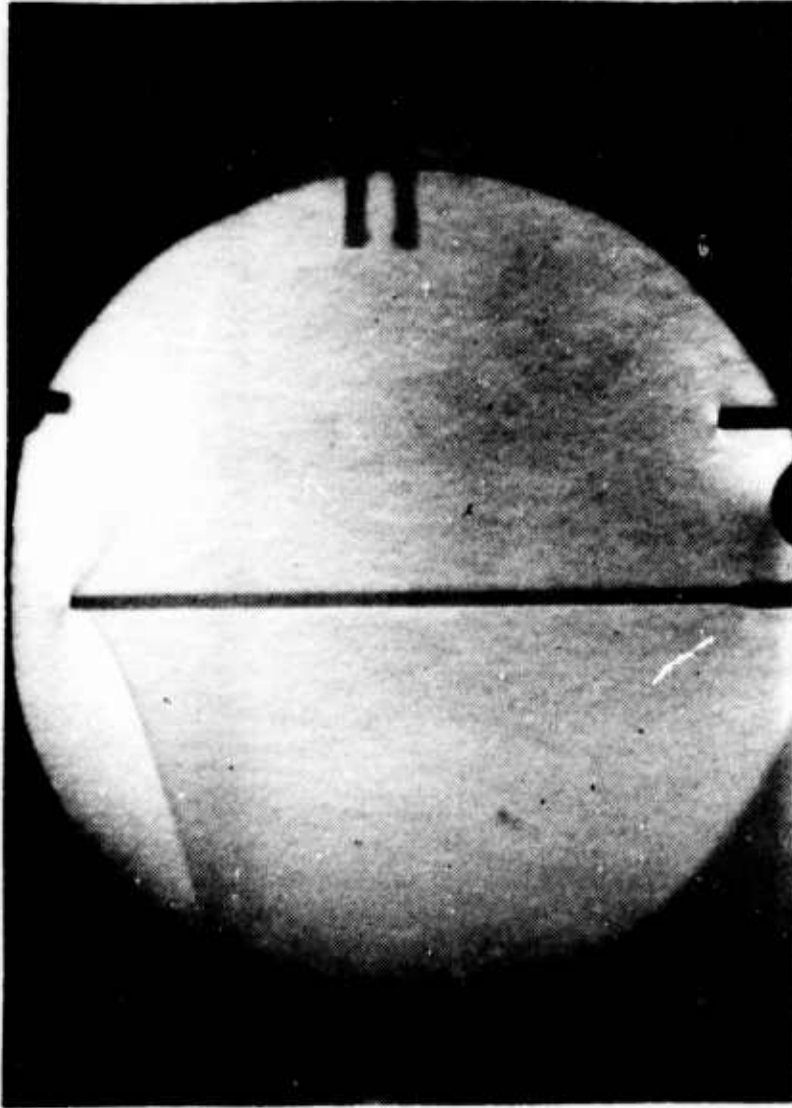
Position error measurements were subsequently repeated during the test program for which the compensation probes were being evaluated. These measurements were made with the (probe mounted on the side of the nose) orifices at stations 6, 7, 9, and 11 inches forward of the nose. Repetition of the position error measurements at subsonic speeds was made to insure that the previous position error test results were valid. In addition, the measurements were extended to Mach 1.15, which is the upper limit of the NSRDC transonic facility. The position error tests were extended to supersonic speeds to determine the extent to which the wind tunnel provides adequate undisturbed ambient pressures, since wind tunnel pressure data is invalid at very low supersonic speeds because of shock reflections from the tunnel walls onto the probe or onto the model which can influence the probe pressure through the subsonic boundary layer. At higher supersonic speeds, shocks of small strength and/or flow nonuniformity can result in differences of static pressure between the tunnel axis and the tunnel tank, where the latter was assumed to be the undisturbed ambient pressure.

The two sets of position error data are in good agreement. The data for the orifices 6, 7, 9, and 11 in. forward of the nose are shown in figure 9. The 11-in. data is accurate for readings of less than 0.5 percent but is in error by as much as 0.5 percent at readings of 2 percent or larger because of a faulty transducer. The 11-in. data is included in the figure because, together with the Schlieren photographs, it helps to clearly show the progress of the bow shock toward the nose with increasing Mach number and does give a measure of the tunnel flow disturbances at supersonic speeds.

The pressures induced by the missile increase with increasing Mach number in a smooth manner at all orifice locations from Mach 0.90 up to and including Mach 1.003, (fig. 9). The data shows no apparent wind tunnel interference or effect of the bow shock up to and including Mach 1.003. Although the Schlieren photograph for Mach 1.003 shows the presence of a shock oscillating between stations 11.5 and 12.5 in. forward of the nose, the shock is apparently too weak to cause any effect, (fig. 10).

The Schlieren photograph at Mach 1.011, (fig. 11), shows the shock oscillating between stations 10 and 12. Here, a break in the pressure rise is observed at station 11, with no effect on the remaining orifices, (fig. 9).

The shock oscillation occurs between stations 9.2 and 10.4 at Mach 1.019, (fig. 12), whereupon the flow at station 11 appears to be entirely supersonic with a pressure corresponding approximately to the undisturbed ambient. The pressure at station 9, located just downstream of the shock, is about 1 percent of the undisturbed ambient larger than that which would have occurred in the absence of the shock, (fig. 9). Similarly, the shock produces increased pressures of about 0.7 and 0.5 percent of the ambient at stations 7 and 6.



Reproduced from
best available copy. 

Figure 10. Position of bow shock on position error probe. $M = 1.003$

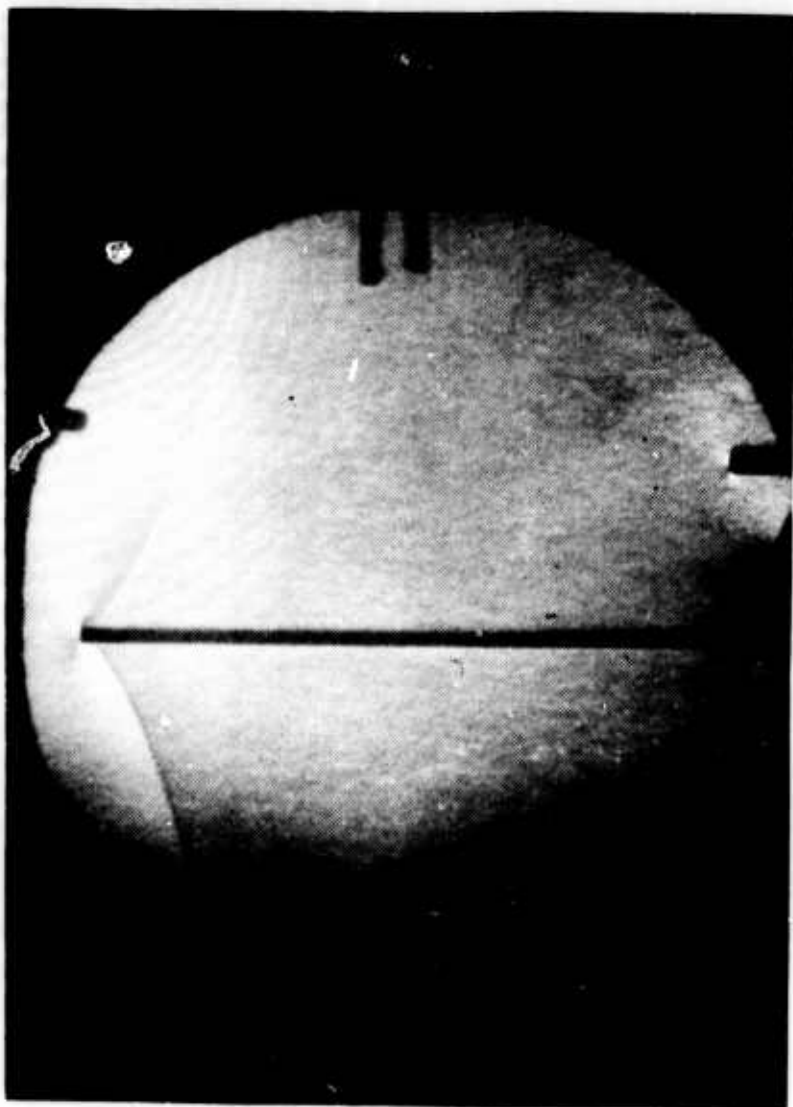


Figure 11. Position of bow shock on position error probe. $M = 1.011$

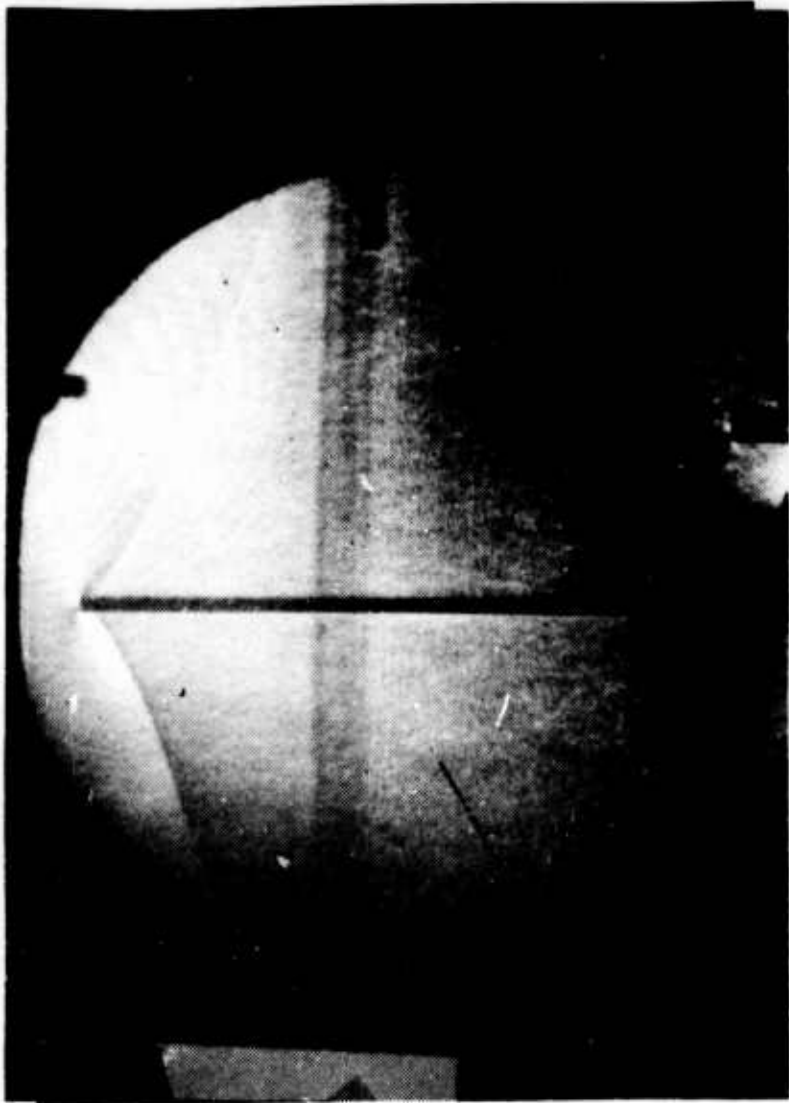


Figure 12. Position of bow shock on position error probe. $M = 1.019$

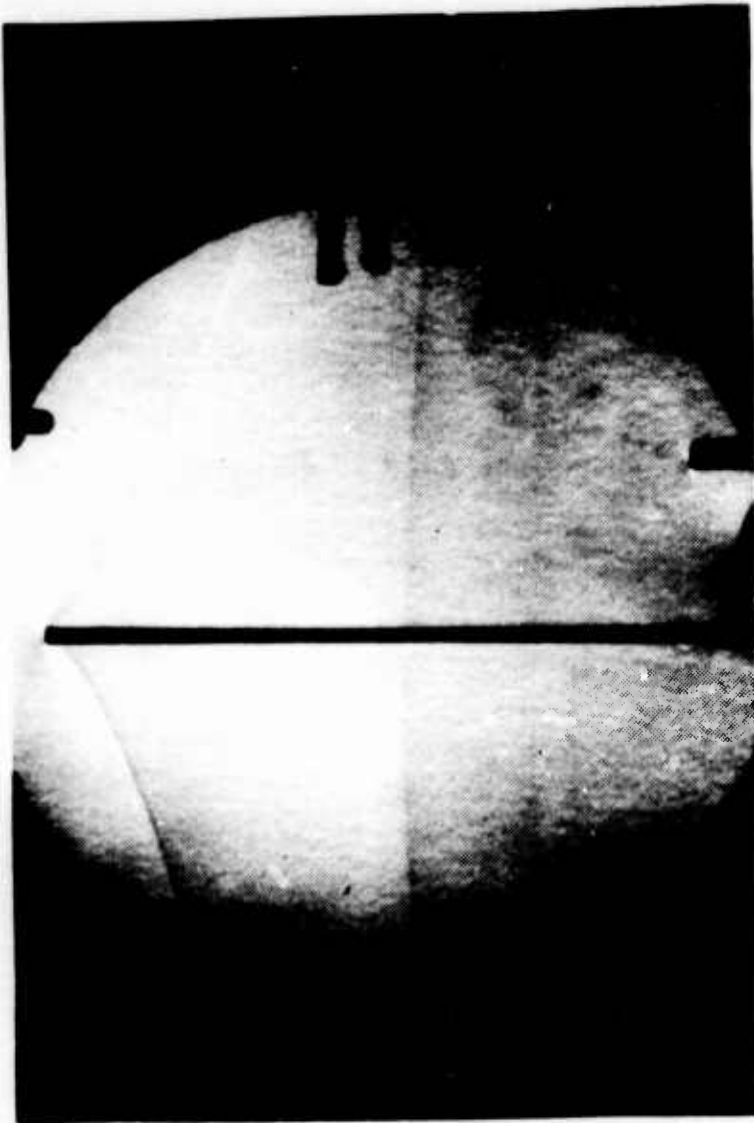
A bow shock oscillates between stations 4.6 and 7.5 at Mach 1.030, (fig. 13), so that the flow at stations 9 and 11 is entirely supersonic with pressures corresponding approximately to the undisturbed ambient. The shock produces an approximate 0.8 percent increase of the ambient pressure at station 6, (fig. 9). The oscillations of the shock over the orifices at station 7 cause the pressures to tend to an average value which is almost a continuation of the subsonic pressure increase with Mach number for this station. As previously noted, seven readings at 1-sec intervals were recorded for each data point. A review of this data shows that the fluctuations occur too rapidly to be recorded with the present instrumentation. Hence, although pressure fluctuations associated with the shock oscillations are unquestionably present, the system time lag is too large to record them. However, the system time lag is not an important consideration in the design of the present fuze system, since the axial position of the bow shock moves large distances with very small changes in Mach number.

The flow is supersonic at all four orifice locations at Mach 1.049. As shown in the Schlieren photograph, (fig. 14), the bow shock is stationary at station 4.8, well behind all four orifice locations. The tunnel interference is significant (difference between the orifice pressure and the tunnel static exceeds 0.4 percent of the tunnel static for supersonic flow) over the Mach range 1.03 to 1.07. The wind tunnel flow then appears to be satisfactory for the remainder of the supersonic range, except with some correction needed for Mach numbers between 1.134 and 1.151 where pressure disturbances of about ± 0.5 percent of the tunnel static appear.

The pressure error measurements given in figures 8 or 9 establish the requirements for the compensation probes.

3.2 Compensation Probe Measurements

At subsonic speeds, because of the local increase of speed, pressures lower than the undisturbed free stream ambient occur over the nose region of highly streamlined bodies of revolution. Pressure data on this type of body is readily available, (refs 5-20). The pressure difference between the undisturbed ambient and body value decreases with increased streamlining of the body. For selected orifice locations on highly streamlined bodies, the body pressure becomes approximately equal to the undisturbed ambient over a range of supersonic speeds. The required pressure variation with Mach number for the compensation probe is the negative of that given by the pressure error measurements shown in figures 8 or 9 for several locations of the orifices forward of the nose of the Honest John Missile. As previously stated, the accuracy with which the ambient pressure can be measured improves as the orifices are moved further forward of the nose.



Reproduced from
best available copy. 

Figure 13. Position of bow shock on position error probe. $M = 1.030$

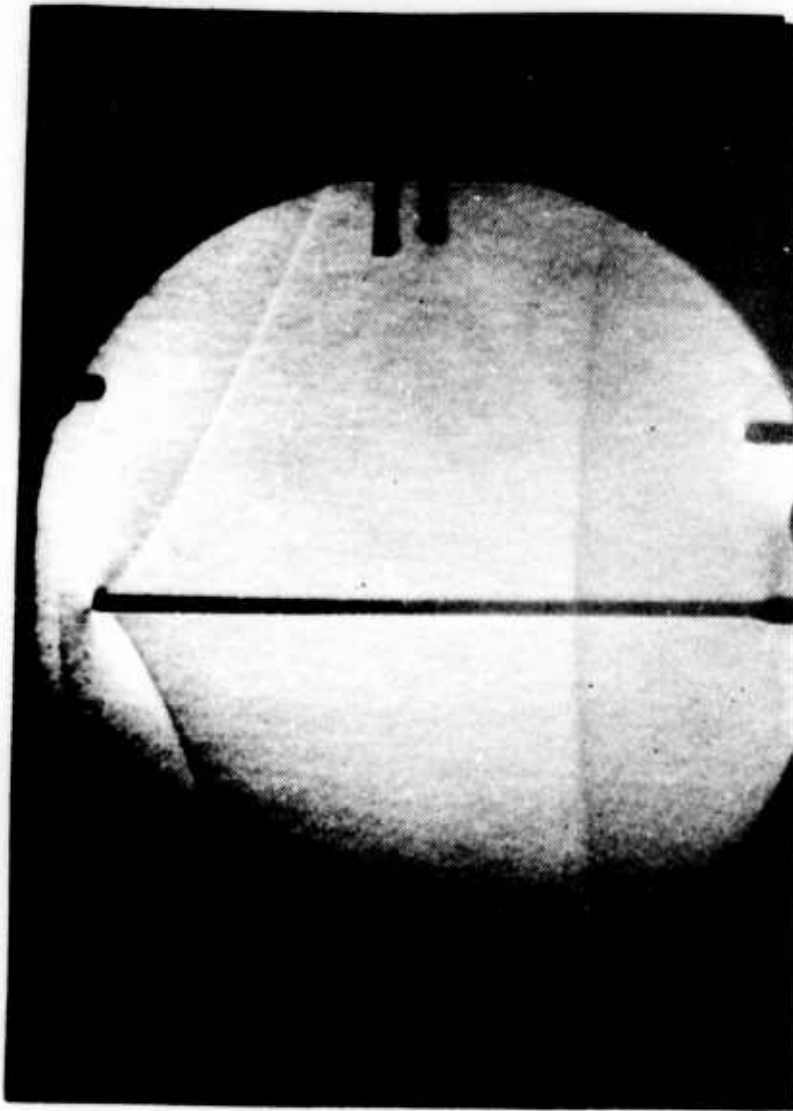


Figure 14. Position of bow shock on position error probe. $M = 1.049$

Each compensation probe measurement was obtained using three transducers teed into a common channel connecting the ring or rings of the orifices, with the tip of the probe extending 12 inches forward of the vehicle nose. The output of each transducer was individually obtained and the reduced data compared with each other to minimize possible error in the data. As with the position error measurements, seven readings at 1-sec intervals were recorded for each data point along with Schlieren photographs. The data is presented in the form of P as a function of M for each of the probes in figures 15A - 15C. Each symbol o, x, + refers to a specific transducer. As shown, the reduced data from the three transducers agrees to within ± 0.1 percent of the pressure value for each data point and each probe, which is well within the ± 0.5 percent maximum error limits of each transducer.

Typical for each probe, the quantity P varies smoothly with M over the range 0.90 to about 1.01, at which speed an oscillating bow shock is located a short distance forward of the orifices and causes an increase in the pressure at the orifices of each probe. At low supersonic speeds, there will tend to be some effect of the probe nose shape on the bow shock oscillation and its position at a given Mach number, since the bow shock position is highly unstable and travels several inches in the direction toward the vehicle nose as the speed increases from 1.00 to 1.02. However, within a difference of Mach number less than 0.01, the bow shock behavior for the compensation and position error probes is essentially the same. Moreover, the differences between the nose shapes of the three compensation probes were not sufficient to significantly affect the position of the bow shock or the Mach number at which it appeared. For each probe, the bow shock produces a pressure increase of between 0.4 and 0.5 percent of the static pressure at Mach 1.01.

The real-time output of each transducer was displayed and consequently it was possible to observe the probe pressure as the tunnel speed was changed. The pressure increases caused by the bow shock shown in figures 15A - 15C are the maximum that could be observed. The pressure increase appeared only over a Mach number range of less than 0.01, because of the large travel of the bow shock with Mach number.

A marked decrease in pressure occurs immediately following the bow shock passage over the orifices in the direction towards the vehicle nose. These pressure decreases are shown in figures 15A - 15C and occur for each of the three compensation probes at between Mach 1.02 and 1.01. The bow shock is of sufficient strength (ratio of pressures immediately aft to forward of shock) to produce tunnel wall boundary-reflected shocks and expansion waves that affect the pressures at the probe orifices. The reduction in pressure arises from the flow expansion produced by the model-tunnel interference. Of course, these reflected shocks and flow expansions would not occur in flight, and all such data is invalid over

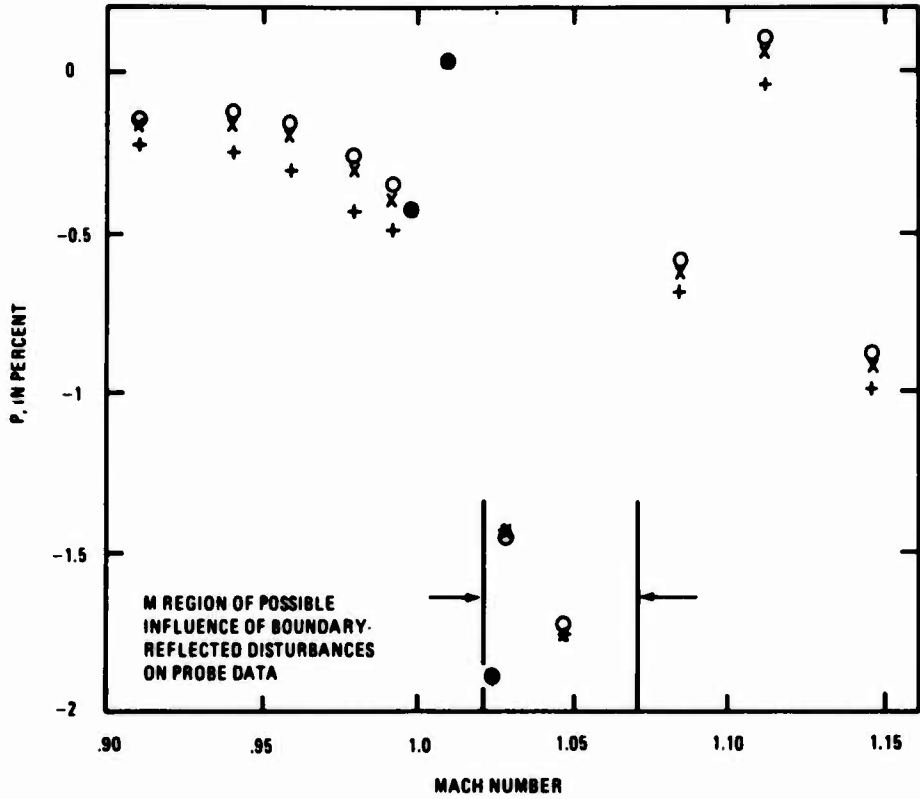


Figure 15A. Error in measuring undisturbed free stream ambient pressure. Probe A

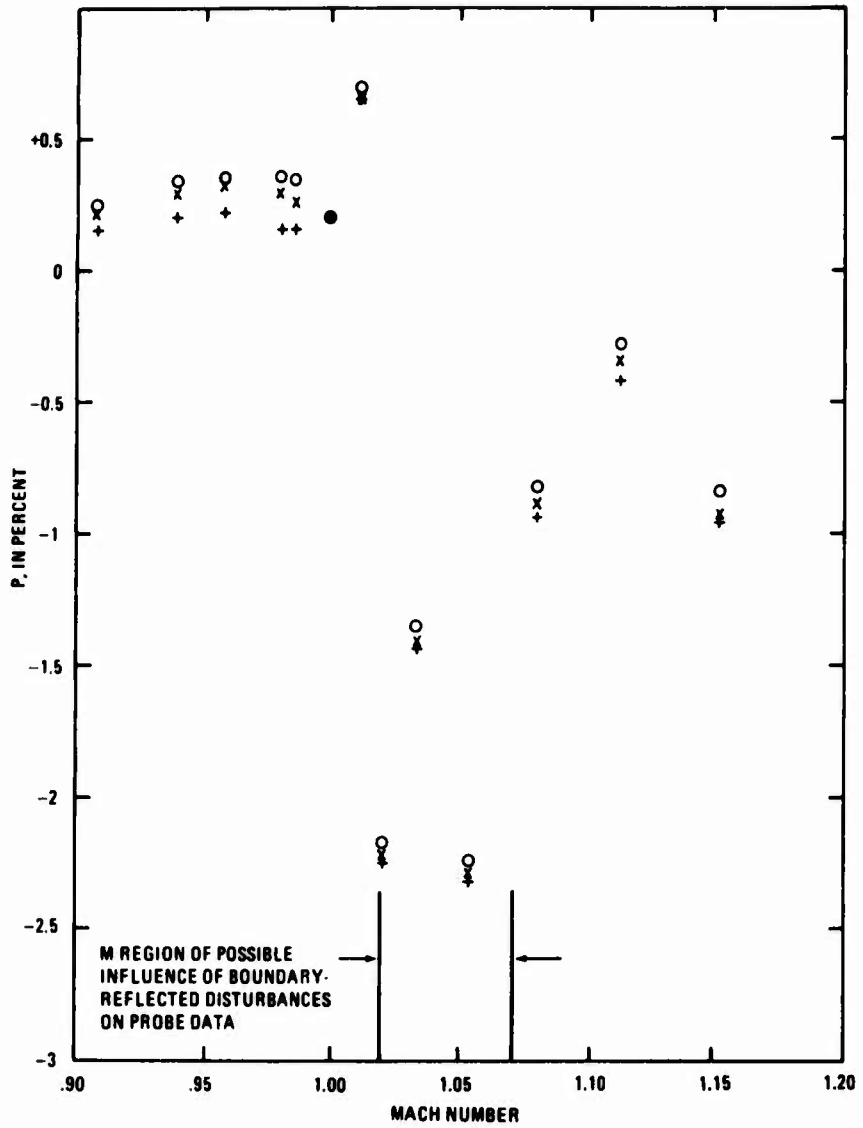


Figure 15B. Error in measuring undisturbed free stream ambient pressure. Probe B

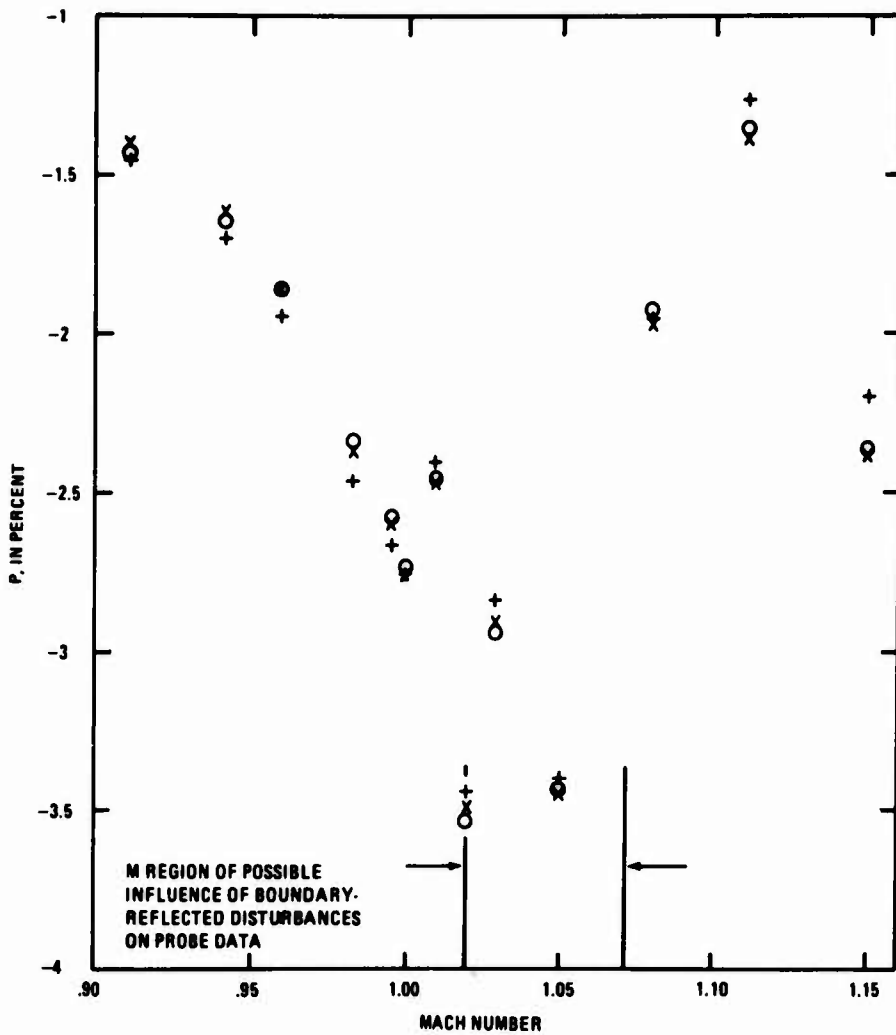


Figure 15C. Error in measuring undisturbed free stream ambient pressure. Probe C

the Mach number range for which they occur. Since the appearance of the bow shocks for the position error probe is essentially identical to that on the compensation probes, the position error data can be used to indicate the Mach number limits for which wind tunnel interference will affect the probe data. As previously noted in figure 9, the position error data indicates tunnel interference over the range 1.03 to 1.07 and some pressure nonuniformities between 1.13 and 1.15. This result is in agreement with the compensation probe data shown in figures 15A - 15C, where marked decreases in the probe pressures occur in the range 1.02 to 1.06. Consequently, the compensation probe data was assumed invalid for the Mach range 1.02 to 1.07. In addition, the compensation probe data at Mach 1.15 was corrected by the amount of the tunnel error indicated for the speed by the position error data; namely the ratio P for each compensation probe was increased by 0.5 percent.

As shown in figures 15A - 15C, with the above corrections, the data envelopes for P (defining the maximum and minimum differences between the probe and undisturbed ambient pressures) are given by +0.1 and -0.6 percent for probe A, +0.7 and -0.9 percent for probe B, and -1.3 and -2.6 percent for probe C. Thus, the total variations of P for the three probes amount to +0.35, +0.8, and +0.65 percent, respectively. If we exclude the small speed range of less than 0.01 in Mach number for which the bow shock affects the orifice pressure, the envelope P for probe B is improved to 0.4 and -0.9 percent for a total variation of +0.65 percent.

As indicated by the position error measurements of figure 9, the value of P will increase as the probe orifices are moved closer to the nose of the missile for the Mach range 0.90 to 1.01. At higher supersonic speeds, Reynolds number effects may produce pressure variations at stations near the vehicle nose. Otherwise, except for a very small change of Mach number denoting the passage of the bow shock, relocating the probe orifices will not affect P at supersonic speeds. No reduction in the envelope of P for probe A would be obtained by relocating the orifices. Moving the orifices away from the nose of the missile a distance of approximately 2 in. could reduce the total variation of P for probe B to values to within +0.4 percent. Because the quantity $\partial^2 P / \partial M^2 > 0$ increases with decreasing distance from the nose for Mach numbers between 0.90 and 1.01 (fig. 9), a similar improvement in the variation of P to within +0.5 percent would occur for probe C by moving the orifices toward the missile nose. However, because of the limited wind tunnel testing time and since the tunnel test conditions corresponded to about 40,000 ft rather than the required sea level to 5,000 ft altitude, data was not obtained for various probe positions.

The value for P may be made more positive at supersonic speeds by blunting the nose of the compensation probes, figure 22 of reference 5. The variation of P for probes A and B appears to be as large or larger at supersonic speeds than at subsonic speeds. Consequently, within the P

variation defined by the supersonic speed range, the positions of probes A and B may be changed somewhat without affecting the P variation for the entire Mach range 0.9 to 1.15. However, the final determination of the probe position must also take into account the distribution of speeds of the missile at which fuzing is required. In this way, a distribution for the system fuzing error can be obtained and the probe position can be shifted to optimize this distribution with respect to minimizing the maximum error, minimizing the average error and so forth.

4. SUMMARY

(a) Position error and compensation probe measurements were conducted at the NSRDC 7 x 10 ft transonic wind tunnel facility over the Mach number range 0.90 to 1.15 at an approximate Reynolds number per foot of 1.92 million, the latter corresponding to an altitude of approximately 40,000 ft. Although wind tunnel interference effects made the measurements invalid for the Mach range 1.02 to 1.07, the variations obtained for P can be assumed applicable over the entire test range.

(b) Position error measurements in the region 5 to 10 in. forward of the vehicle nose show that a predicted rise in static pressure caused by simultaneous 5 degree canard and 10 degree afterbody deflections amounted to only about 0.1 to 0.2 percent of the static pressure through the Mach range 0.90 to 1.00; no effect occurs for $M \geq 1.05$. Consequently, all evaluations of the compensation probes can be made at a single configuration of the vehicle.

(c) The bow shock caused a maximum increase in static pressure on the compensation probes of 0.5 percent, and its influence was noted over a Mach range of less than 0.01.

(d) The compensation probe pressures at sea level conditions can be expected to be only slightly changed from those obtained in the present tests. Consequently, it is expected that any necessary changes in probe performance can be obtained by making small changes in the amount the probe extends beyond the seeker nose and without any change of the probe itself. The coordinates of the three probes are considered final, as given.

(e) When the compensation probes are mounted in the position forward of the vehicle to yield the smallest overall variations of P, it is expected that these variations for probes A, B, and C will be ± 0.35 , ± 0.4 , and ± 0.5 percent of the undisturbed ambient pressure, respectively. This accuracy is consistent with the results reported in reference 5. Since a 1 percent change in pressure corresponds to an altitude change of

275 ft. and allowing for 0.1 percent error in prediction of the pressure-altitude relation, 0.25 percent error in the barometric switch and the above probe errors, for altitudes between sea level and 5,000 ft, the fuze system error is not expected to exceed 120, 130, and 160 ft for probes A, B, and C, respectively. The error distribution and standard deviation for the fuzing system cannot be given, since no information is available regarding the distribution for the missile speed.

(f) Since Reynolds number effects are not actually known for compensation probes on blunt-nosed vehicles, and since it is only assumed that the present results can be extended without error from Mach 1.15 to 1.20, it is recommended that the compensation probes be evaluated on the full-scale model of the forward section of the Honest John Missile at sea level flight conditions, as is possible in the NASA Ames 11 x 11 ft transonic wind tunnel facility. Because of its larger size, this facility can also be expected to introduce a smaller Mach range of wind tunnel interference on the model, compared with the interference found between Mach 1.02 and 1.07 in the NSRDC facility. These wind tunnel tests would be sufficient to complete the evaluation of the probes and free flight tests may not be required.

SYMBOLS

- M free stream Mach number
- p local static pressure (sensed by probe), psi
- p[∞] free stream static pressure, psi
- $P = \frac{P - P^\infty}{p}$ error in measuring free stream static pressure
- x axial distance from tip of probe nose, inch
- y distance from centerline of probe to surface of probe, inch

LITERATURE CITED

1. Brauer, R. C., "A Method of Calculating the Response Time of Pressure Measuring Systems," AEDC-TR-56-7 (Nov 1956), Astia Document No. AD 98978.
2. Huston, W. B., "Accuracy of Airspeed Measurements and Flight Calibration Procedures," NACA TR-919 (1948).
3. Sinclair, A. R. and Robins, A. W., "A Method for the Determination of the Time Lag In Pressure Measuring Systems Incorporating Capillaries," NACA TN-2793 (1952).
4. Minibar Baroswitches, Friez Instrument Division, Bendix Aviation Corporation, Towson, Maryland.
5. Ritchie, V. S., "Several Methods for Aerodynamic Reduction of Static-Pressure Sensing Errors for Aircraft at Subsonic, Near-Sonic, and Low Supersonic Speeds," NASA TR R-18 (1959).
6. Harris, R. V., Jr., and Landrum, E. J., "Drag Characteristics of a Series of Low-Drag Bodies of Revolution at Mach Numbers From 0.6 to 4.0," NASA TND-3163 (1965).
7. Estabrooks, B. B., "An Analysis of the Pressure Distribution Measured on a Body of Revolution at Transonic Speeds in the Slotted Test Section of the Langley 8-Foot Transonic Tunnel," NACA RM L52D21a (1952).
8. Robinson, H. L., "Pressures and Associated Aerodynamic and Load Characteristics for Two Bodies of Revolution at Transonic Speeds," NACA RM L53L28a (1954).
9. Capone, F. J., "Wind-Tunnel Tests of Seven Static-Pressure Probes at Transonic Speeds," NACA TN D-947 (1961).
10. Brunn, C. D., and Stillwell, W. H., "Mach Number Measurements and Calibrations During Flight at High Speeds and at High Altitudes Including Data for the D-558-II Research Airplane," NACA RM H55J18 (1956).

11. Homan, M. L., "Calibration of Two Aerodynamically Compensated Pitot-Static Probes for the F-111B Aircraft at Mach Numbers From 0.7 to 1.5," AEDC-TR-68-207 (1968), DDC AD No. 840936.
12. Barnes, C. S., and Nicholas, O. P., "Flight and Wind-Tunnel Tests on an Aerodynamically Compensated Pitot-Static Head for the BAC 221 Aircraft," R.A.E. TR-69013 (1969), DDC AD No. 856994.
13. Perkins, T. M. and Brice, T. R., "Transonic Wind-Tunnel Tests of a Conical and a Hemispherical Probe," AEDC-TR-66-29 (1966), DDC AD No. 476895.
14. White, W. E. "Transonic Wind-Tunnel Tests of Three Pitot-Static Probes Designed for Pressure-Error Compensation on the RF-4C (RF-110) Aircraft," AEDC TDR-63-220 (1963), DDC AD No. 419124.
15. Capone, F. J., "Transonic Wind-Tunnel Tests of an Error-Compensated Static-Pressure Probe," NASA TN D-961 (1961).
16. Price, E. A., Jr., "Calibration of an Aerodynamically Compensated Pitot-Static Probe for the RF-4C Aircraft at Mach Numbers From 0.5 to 1.2," AEDC-TR-67-153 (1967), DDC AD No. 817166.
17. Kukainis, J., "Calibration of an Aerodynamically Compensated Pitot-Static Probe for the RF-101 Aircraft at Mach Numbers From 0.5 to 1.5," AEDC-TR-67-270 (1967), DDC AD No. 824390.
18. Kuklewicz, E. F., "Transonic Wind-Tunnel Tests of Two Prototype Pitot-Static Pressure Probes," David Taylor Model Basin Test Report AL-24 (1966), DDC AD No. 480381.
19. Sandler, S. H. and Kuklewicz, E. F., "Transonic Wind-Tunnel Tests of Static Pressure Probes Designed to Sense Free-Stream Static Pressure," David Taylor Model Basin Test Report AL 8 (1964), DDC AD No. 454644.
20. Perkins, T. M. and Black, A., "Transonic Wind-Tunnel Test of Two Pitot-Static Probes Designed for Pressure-Error Compensation on the RF-4C (RF-110) Aircraft," AEDC-TDR-64-44 (1964), DDC AD No. 431534.
21. Thomas, W. S., David Taylor Model Basin 7 x 10 ft Transonic Wind Tunnel Facility, Aero Report 985, July 1960.
22. Chaddock, Dale, (Report in Preparation Describing David Taylor Model Basin New Wind Tunnel Survey).
23. Braslow, A. L., and Knox, E. C. "Simplified Method for Determination of Critical Height of Distributed Roughness Particles for Boundary-Layer Transition at Mach Numbers from 0 to 5," NACA TN 4363 (1958).

24. Cole, C. F., "The Effects of Some Variations in Launch-Vehicle Nose Shape on Steady and Fluctuating Pressures at Transonic Speeds," NASA TM X-6461 (March 1962), DDC AD No. 328 202.
25. Robertson, J. E., and Chevalier, H. L., "Characteristics of Steady-State Pressures on the Cylindrical Portion of Cone-Cylinder Bodies at Transonic Speeds," Tech. Doc. Rpt. No. AEDC-TDR-63-104 (August 1963), DDC AD No. 413535.
26. Matthews, C. W., "A Comparison of the Experimental Subsonic Pressure Distributions About Several Bodies of Revolution with Pressure Distributions Computed by Means of the Linearized Theory," NASA TR-1155 (1953).
27. Gardiner, G. K., "Wind Tunnel Calibration Tests and Pressure Measurements on a Blunted Slender Cone from Mach 0.3 to 1.3," Litton Systems, Inc., HADES-R-65-1, Vol I (Jan 1965), DDC AD No. 461744.
28. Robertson, J. E., "Steady and Fluctuating Pressures on Cone-Cylinder Missile Configurations at Transonic Speeds," AEDC-TR-65-269 (Feb. 1966), DDC AD No. 477938.
29. Chevalier, H. L., and Robertson, J. E., "Pressure Fluctuations Resulting from an Alternating Flow Separation and Attachment at Transonic Speeds," AEDC-TDR-63-204 (Nov 1963), DDC AD No. 423095.

APPENDIX
PROBE COORDINATES

PROBE A

x, in.	y, in.
0	0
.023	.0104
.034	.0134
.056	.0193
.113	.0325
.225	.0542
.338	.0726
.450	.0887
.675	.1166
.900	.1390
1.125	.1559
1.350	.1684
1.575	.1770
2.025	.1865
2.250	.1875

PROBE B

x	y
0	0
.0185	.0080
.0370	.0130
.0556	.0180
.0745	.0225
.0930	.0265
.1115	.0305
.1300	.0340
.1485	.0375
.1670	.0405
.1855	.0440
.2785	.0590
.3715	.0725
.5570	.0965
.7425	.1170
.9280	.1355
1.1140	.1520
1.2995	.1675
1.4850	.1810
1.6710	.1930
1.8565	.2040
2.0420	.2135
2.2275	.2220
2.4135	.2300
2.5990	.2365

x	y
2.7845	.2425
2.9705	.2470
3.1560	.2505
3.3415	.2535
3.5270	.2555
3.7130	.2565
3.8985	.2570
4.0840	.2565
4.270	.2555
4.4555	.2530
4.6410	.2500
4.8265	.2465
5.0125	.2420
5.1980	.2370
5.3835	.2315
5.5695	.2250
5.755	.2185
5.9405	.2115
6.1260	.2040
6.2190	.2005
6.3120	.1970
6.4045	.1940
6.4975	.1910
6.5905	.1890
6.6830	.1875

PROBE C

x	y
3.903	.1623
4.203	.1649
4.503	.1676
5.003	.1719
5.503	.1763
6.003	.1807
6.503	.1850
6.772	.1874
7.000	.1875